# Image Integration to Guide Catheter Ablation in Scar-Related Ventricular Tachycardia

Seigo Yamashita, Frédéric Sacher, Saagar Mahida, Benjamin Berte, Han S Lim, Yuki Komatsu, Sana Amraoui, Arnaud Denis, Nicolas Derval, François Laurent, et al.

# Image Integration to Guide Catheter Ablation in Scar-Related Ventricular Tachycardia

SEIGO YAMASHITA, M.D., PH.D.,* FRÉDÉRIC SACHER, M.D., PH.D.,*,‡ SAAGAR MAHIDA, M.B.CH.B., PH.D.,* BENJAMIN BERTE, M.D.,* HAN S. LIM, M.B.B.S., PH.D.,* YUKI KOMATSU, M.D.,* SANA AMRAOUI, M.D.,* ARNAUD DENIS, M.D.,*,‡ NICOLAS DERVAL, M.D.,*,‡ FRANÇOIS LAURENT, M.D.,†,‡ MAXIME SERMESANT, PH.D.,§ MICHEL MONTAUDON, M.D., PH.D.,†,‡ MÉLÈZE HOCINI, M.D.,*,‡ MICHEL HAÏSSAGUERRE, M.D., PH.D.,*,‡ PIERRE JAÏS, M.D., PH.D.,*,‡ and HUBERT COCHET, M.D., PH.D.†,‡

From the *Department of Cardiac Electrophysiology, Hôpital Cardiologique du Haut-Lévêque, CHU de Bordeaux, Pessac, France; †Department of Cardiovascular Imaging, Hôpital Cardiologique du Haut-Lévêque, CHU de Bordeaux, Pessac, France; ‡IHU LIRYC-Equipex MUSIC, Université de Bordeaux-Inserm U1045, Pessac, France; and §Inria, Asclepios team, Sophia Antipolis, France

**Image Integration-Guided VT Ablation.** ***Background:*** **Although multi-detector computed tomography (MDCT) and cardiac magnetic resonance (CMR) can assess the structural substrate of ventricular tachycardia (VT) in ischemic cardiomyopathy (ICM), non-ICM (NICM), and arrhythmogenic right ventricular cardiomyopathy (ARVC), the usefulness of systematic image integration during VT ablation remains undetermined.**

***Methods and Results:*** **A total of 116 consecutive patients (67 ICM; 30 NICM; 19 ARVC) underwent VT ablation with image integration (MDCT 91%; CMR 30%; both 22%). Substrate was defined as wall thinning on MDCT and late gadolinium-enhancement on CMR in ICM/NICM, and as myocardial hypoattenuation on MDCT in ARVC. This substrate was compared to mapping and ablation results with the endpoint of complete elimination of local abnormal ventricular activity (LAVA), and the impact of image integration on procedural management was analyzed. Imaging-derived substrate identified 89% of critical VT isthmuses and 85% of LAVA, and was more efficient in identifying LAVA in ICM and ARVC than in NICM (90% and 90% vs. 72%, $P < 0.0001$), and when defined from CMR than MDCT (ICM: 92% vs. 88%, $P = 0.026$, NICM: 88% vs. 72%, $P < 0.001$). Image integration motivated additional mapping and epicardial access in 57% and 33% of patients. Coronary and phrenic nerve integration modified epicardial ablation strategy in 43% of patients. The impact of image integration on procedural management was higher in ARVC/NICM than in ICM ($P < 0.01$), and higher in case of epicardial approach ($P < 0.0001$).**

***Conclusions:*** **Image integration is feasible in large series of patients, provides information on VT substrate, and impacts procedural management, particularly in ARVC/NICM, and in case of epicardial approach.** *(J Cardiovasc Electrophysiol, Vol. 27, pp. 699-708, June 2016)*

*ablation, CMR, MDCT, imaging, scar-related ventricular tachycardia*

## Introduction

Radiofrequency (RF) ablation is an effective treatment strategy for ischemic (ICM) and non-ischemic cardiomyopathy (NICM) patients with ventricular tachycardia (VT). The role of substrate-based techniques for VT ablation is expanding, including targeting the electrophysiological (EP) substrate as indicated by the presence of local abnormal ventricular activity (LAVA).[1-3] Integration of multi-detector computed tomography (MDCT) and late gadolinium-enhancement cardiac magnetic resonance (LGE-CMR) imaging during VT ablation has demonstrated promise in preliminary studies.[4-7] However, studies to date have been restricted to small numbers of patients, and the impact of image integration on procedural management has not been thoroughly studied.

The aim of this study was to report on the systematic use of image integration for scar-related VT ablation. Specific objectives were: (i) to describe a method for data preparation and procedural use and demonstrate feasibility in clinical practice, (ii) to report on the performance of imaging in identifying EP substrate according to specific VT etiology, and (iii) to analyze the impact of imaging on the procedural management.

## Methods

### *Study Population*

From January 2012 to December 2013, consecutive patients with drug-refractory, scar-related VT who were referred for catheter ablation were included. Patients with contra-indications to both iodine-enhanced MDCT and

The study was funded by l'Agence Nationale de la Recherche (ANR) under Grant Agreements Equipex MUSIC ANR-11-EQPX-0030, MIGAT ANR-13-PRTS-0014-01, and IHU LIRYC ANR-10-IAHU-04.

Disclosures: None.

Address for correspondence: Seigo Yamashita, M.D., Ph.D., Department of Cardiac Electrophysiology, Hôpital Cardiologique du Haut-Lévêque Avenue de Magellan, 33604, Bordeaux-Pessac, France. Fax: 33-5-57-65-64-19; E-mail: seigoy722@yahoo.co.jp

Manuscript received 9 August 2015; Revised manuscript received 27 January 2016; Accepted for publication 15 February 2016.

doi: 10.1111/jce.12963

gadolinium-enhanced CMR were excluded. ICDs were considered as a contra-indication to CMR. The VT etiology was categorized as ICM, arrhythmogenic right ventricular cardiomyopathy (ARVC), or other forms of NICM. ARVC was diagnosed based on 2010 Task Force criteria.[8] This study was approved by the institutional review board, and all patients gave informed consent.

### *Image Acquisition*

Imaging was performed 1–3 days before the ablation procedure. Contrast-enhanced ECG-gated cardiac MDCT and CMR were performed on a 64-slice CT scanner (SOMATOM Definition, Siemens Medical Solutions, Forchheim, Germany) and 1.5 T system (Avanto, Siemens Medical Solutions, Erlangen, Germany) as reported previously.[6,9] Briefly, MDCT was acquired during the injection of 120 mL iomeprol (400 mg I/mL, Bracco, Milan, Italy) using a biphasic injection protocol. LGE image on CMR was acquired 15 minutes after the intravenous injection of 0.2 mmol/kg gadoterate meglumine (Guerbet, Aulnay-sous-bois, France), using a free-breathing method initially developed for atrial imaging (voxel size 2.5 × 1.25 × 1.25 mm). Both images were reconstructed into a stack of 1-mm-thick slices in short axis orientation.

### *Image Analysis and Processing*

Image processing was performed by 2 technicians using the MUSIC software (Liryc-Université de Bordeaux/Inria-Sophia Antipolis, France). Segmentation was performed as described previously.[6,10-12] Briefly, the cardiac chambers, ventricular epicardium, ascending aorta, and coronary sinus (CS) were segmented using semi-automatic methods.[10] In patients undergoing epicardial procedures, additional segmentation was performed to extract the coronary arteries (CAs) and left phrenic nerve (PN).[11] In case both CMR and MDCT had been performed, datasets were registered prior to segmentation.[10] In ICM and NICM, the structural substrate was defined as wall thinning (WT) on MDCT and LGE on CMR. To provide anatomical substrate heterogeneity, WT areas were divided into severe WT (<2 mm) and moderate WT (2–5 mm),[6] and LGE areas were divided into dense scar (>50% maximum signal intensity) and gray zone (35–50% maximum signal intensity).[13,14] In ARVC, CMR could be used for diagnostic purposes but was not considered for image integration because of spatial resolution limitations in assessing the thin RV wall. In these patients the structural substrate was only defined from MDCT as areas of myocardial hypo-attenuation (HA) (←10 HU).[12,15] All segmented structures were exported in the form of 3D meshes and loaded into 3D mapping systems (Ensite NavX, St. Jude Medical Inc, St. Paul, MN, USA or CARTO3, Biosense Webster, Inc., Diamond Bar, CA, USA) prior to the EP procedure.

### *Electrophysiological Mapping Study and Image Integration*

A steerable catheter (2–5–2 mm, Xtrem, ELA Medical, Montrouge, France; Dynamic, Boston Scientific, Natick, MA, USA) was positioned in the right ventricular (RV) apex or CS. The left ventricle (LV) was accessed by transseptal (BRK Needle, St. Jude Medical) and/or retrograde approach with or without pericardial access (Tuohy needle and Agilis sheath, St. Jude Medical).[16] Unless contra-indicated, an epicardial approach was performed in VTs with a suspected epicardial origin based on imaging (subepicardial or transmural LGE on CMR,[17] subepicardial HA[12] on MDCT), 12-lead ECG, absence of LAVAs on the endocardium, and/or the persistence of clinical VT after endocardial ablation. Imaging was used as an additional criterion to indicate an epicardial approach, but was not used to contra-indicate such an approach. Electroanatomical mapping (EAM) was performed during sinus rhythm (SR). An irrigated catheter with 3.5-mm-tip and/or multipolar high-density mapping catheter (NaviStar ThermoCool and/or PentaRay, Biosense Webster) were used for mapping. A peak-to-peak amplitude <1.5 mV of bipolar voltage defined the low voltage zone (LVZ).

Image registration was performed after mapping and prior to ablation.[6,10] Anatomical landmarks were used to initiate point-based registration between the imaging and mapping geometries. When using NavX platform, registration was refined using field scaling and additional landmarks on LV and/or RV free walls. When using CARTO platform, registration was refined using automatic surface registration and the accuracy was assessed by surface registration error. In addition, a 6 F-quadripolar or decapolar catheter was placed into the distal CS in an anterior or lateral vein to detect a potential shift of the map registration throughout the procedure.[10,11] After acquisition of an integrated image, additional mapping focusing on the anatomical substrate area (WT, HA area on MDCT, and LGE area on CMR) was performed if necessary. The agreement between imaging substrate (WT<5 mm[6] or HA←10 HU[12] on MDCT, LGE>35% signal intensity[13] on CMR) and LVZ was expressed as the area of overlap, expressed in % of the total imaging substrate and LVZ area on both endo- and epicardium. False-positive and false-negative areas were also measured, using the imaging substrate (WT-MDCT/LGE-CMR) as a reference.

### *Catheter Ablation and Outcome*

VT inducibility was assessed with 2 drive trains (600 milliseconds and 400 milliseconds) with up to 3 extrastimuli decremented to 200 milliseconds from the RV apex. In patients with 0.0 inducible and tolerated VT, a VT map was acquired and ablation was performed with the guidance of the conventional activation and entrainment mapping. After restoration of SR, ablation of LAVA was performed with the endpoint of LAVA elimination.[2] In cases with non-inducible VT and/or VT that was not tolerated, LAVA was targeted during SR or ventricular pacing. RF power was limited to 25–50 W endocardially and 25–35 W epicardially. In case with epicardial ablation, when LAVA were located <5 mm from the left PN and CAs on the integrated image, the decision to deliver RF energy was based on pacing with maximum output and coronary angiography. Patients were followed up postprocedure with regular ICD interrogations (1, 3, 6, and 12 months for the first year and subsequently every 6 months) or remote monitoring system (46% in this study). In patients without ICD, Holter monitoring was performed whenever an arrhythmic event was suspected. The primary endpoint was VT recurrence.

### *Impact of Imaging on the Procedural Management*

In order to determine the impact of image integration on the procedure the operator was asked to provide feedback on the following points: (i) Did imaging specifically motivate an

**TABLE 1**
Patients' Characteristics

| | Total (n = 116) | ICM (n = 67) | NICM (n = 30) | ARVC (n = 19) |
|---|---|---|---|---|
| Age, years | 58 ± 15 | 63 ± 12 | 55 ± 13 | 44 ± 15 |
| Male, n | 109 (94%) | 64 (96%) | 28 (93%) | 17 (90%) |
| LVEF, % | 36 ± 14 | 31 ± 11 | 32 ± 11 | 58 ± 8 |
| LVDD, mm | 63 ± 7 | 64 ± 7 | 61 ± 8 | 52 ± 1 |
| Prior VT ablation, n | 1.4 ± 0.9 | 1.3 ± 1.0 | 1.3 ± 0.6 | 1.7 ± 1.0 |
| ICD, n | 79 (68%) | 40 (60%) | 22 (73%) | 17 (89%) |
| Beta-blocker, n | 109 (94%) | 65 (97%) | 28 (93%) | 16 (84%) |
| Amiodarone, n | 80 (69%) | 48 (71%) | 17 (57%) | 15 (79%) |
| Imaging | | | | |
| MDCT, n | 106 (91%) | 59 (88%) | 28 (93%) | 19 (100%) |
| CMR, n | 35 (30%) | 26 (39%) | 9 (30%) | – |
| Both CT and CMR, n | 25 (22%) | 18 (27%) | 7 (23%) | – |

ARVC = arrhythmogenic right ventricular cardiomyopathy; CMR = cardiac magnetic resonance; MDCT = multi-detected computed tomography; ICD = implantable cardioverter defibrillator; ICM = ischemic cardiomyopathy; LVDD = left ventricular end-diastolic dimension; LVEF = left ventricular ejection fraction; NICM = non-ischemic cardiomyopathy; VT = ventricular tachycardia.

**TABLE 2**
Imaging Results

| | ICM | NICM | ARVC | P-Value* |
|---|---|---|---|---|
| WT on MDCT, n | 58/59 (98%) | 22/28 (79%) | – | 0.004 |
| Severe WT on MDCT, n | 46/59 (78%) | 3/28 (11%) | – | <0.001 |
| WT area on MDCT, $cm^2$ | 53 (29–81) | 26 (16–75) | – | 0.689 |
| LGE on CMR, n | 26/26 (100%) | 8/9 (89%) | – | 0.257 |
| Transmural LGE on CMR | 15/26 (58%) | 1/9 (11%) | – | 0.022 |
| LGE area in CMR, $cm^2$ | 58 (24–75) | 45 (36–53) | – | 0.495 |
| HA on MDCT, n | – | – | 19/19 (100%) | – |
| HA area on MDCT, $cm^2$ | – | – | 107 (56–149) | – |

*Comparison between ICM and NICM. HA = hypo-attenuation; LGE = late gadolinium-enhancement; WT = wall thinning.

epicardial access that led to the identification of LAVA? (ii) Once mapping was considered complete and before moving to the ablation phase of the procedure, did image integration specifically motivate additional mapping that led to the identification of LAVA? (iii) Did image integration modify the epicardial ablation strategy due to the visualization of CAs and/or left PN? These 3 questions were used to score the impact of imaging from 0 to 3 (imaging utility score). A score of 0 was categorized as "not helpful," 1 or 2 as "helpful," and 3 as "extremely helpful."

### *Statistical Analysis*

Quantitative data are expressed as the mean±SD or median [interquartile range (IQR)] based on the distribution of the values. Comparison between groups was analyzed by using unpaired Student's *t*-test or Wilcoxon rank-sum test. Categorical variables were compared using chi-square or Fisher exact tests. The relationship between variables was analyzed by using Pearson or Spearman correlation coefficients. Cox proportional hazards regression models were used for multivariable analysis of the predictors of VT recurrence. All tests were 2-tailed, and $P < 0.05$ was considered significant. Statistical analyses were performed using the MedCalc software package, version 11.2 (Mariakerke, Belgium).

## Results

### *Population Characteristics*

Patient characteristics are summarized in Table 1. The population comprised 116 patients (age 58 ± 15, 7 female). Sixty-seven (58%) had ICM, 19 (16%) had ARVC, and 30 (26%) had NICM. CMR was contra-indicated due to the presence of ICDs in 79 (68%) patients. MDCT was contra-indicated due to the presence of severe renal failure in 9 (8%) patients.

### *Imaging Results*

Imaging results are summarized in Table 2. In ARVC, all 19 patients exhibited HA-MDCT in the RV, and 10 (53%) patients in the LV. In ICM, WT-MDCT was present in 58 (98%) patients (severe WT in 78%), and LGE-CMR was present in all patients (transmural LGE in 58%). In NICM, WT-MDCT was present in 22 (79%) patients (severe WT in 11% and diffuse WT in 25%). Therefore, WT could provide substrate localization in only 15/28 (54%) patients. LGE-CMR was found in 8 (89%) NICM patients (subepicardial LV lateral, 8/9; mid-myocardial septum 1/9; transmural in 1/9). Examples of abnormal structural substrate on imaging are shown in Figure 1.

### *Feasibility of Image Processing and Registration*

Image processing was feasible in all patients with imaging processing time of 30 minutes in case of endocardial approach on MDCT data only, 45 minutes in case of combined endo- and epicardial approach or combined MDCT and CMR data (Fig. 2). All patient-specific cardiac models were successfully loaded within EAM systems. In CARTO cases (n = 81), registration error was 3.9 ± 1.0 mm. In NavX cases (n = 35), 34 ± 15 points were used to align both geometries.

### *Relationship Between Imaging Substrate and Voltage Mapping*

The results of voltage mapping are shown in Table 3. The agreement between imaging substrate and LVZ is illustrated for each VT etiology on MDCT and CMR in Figure 3. For MDCT-defined substrate, the agreement on the endo/epicardium was higher in ICM and ARVC than in NICM (66 ± 14% and 60 ± 16% vs. 13 ± 16%, $P < 0.0001$ and $P < 0.0001$ on endocardium, 60 ± 14% and 68 ± 20% vs. 23 ± 21%, $P < 0.001$ and $P < 0.001$ on epicardium).

For CMR-defined substrate, the agreement between LVZ and imaging substrate was also higher in ICM than in NICM (73 ± 7% vs. 32 ± 12% for epicardium, $P = 0.009$). In ICM, the agreement was higher when using CMR than MDCT on the epicardium (73 ± 7% vs. 60 ± 13%, $P = 0.002$) but not on the endocardium (69 ± 17% vs. 66 ± 14%, $P = 0.62$). In NICM, the agreement did not differ between CMR and MDCT (epicardium: 32 ± 12% vs. 34 ± 7%, $P = 0.83$).

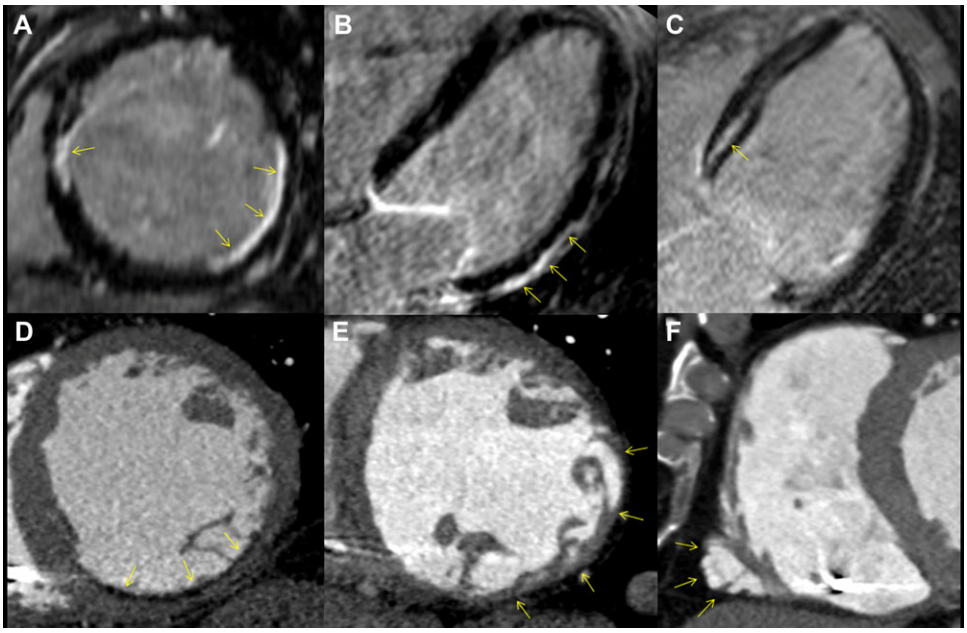


**Figure 1.** *Examples of abnormal structural substrate on imaging. Top row: CMR. A: Subendocardial LGE (arrow) in patient with post-infarction VT. B: Subepicardial LGE (arrow) in post-myocarditis VT patient. C: Mid-wall LGE (arrow) in patient with primitive dilated cardiomyopathy VT. Bottom row: MDCT. D: Inferior WT and subendocardial HA (arrow) in post-infarction VT patient. E: Lateral WT (arrow) in patient with non-ischemic dilated cardiomyopathy. F: Right ventricular aneurysm with HA (arrow) indicating fatty replacement in ARVC patient. For a high quality, full color version of this figure, please see Journal of Cardiovascular Electrophysiology's website: www.wileyonlinelibrary.com/journal/jce*

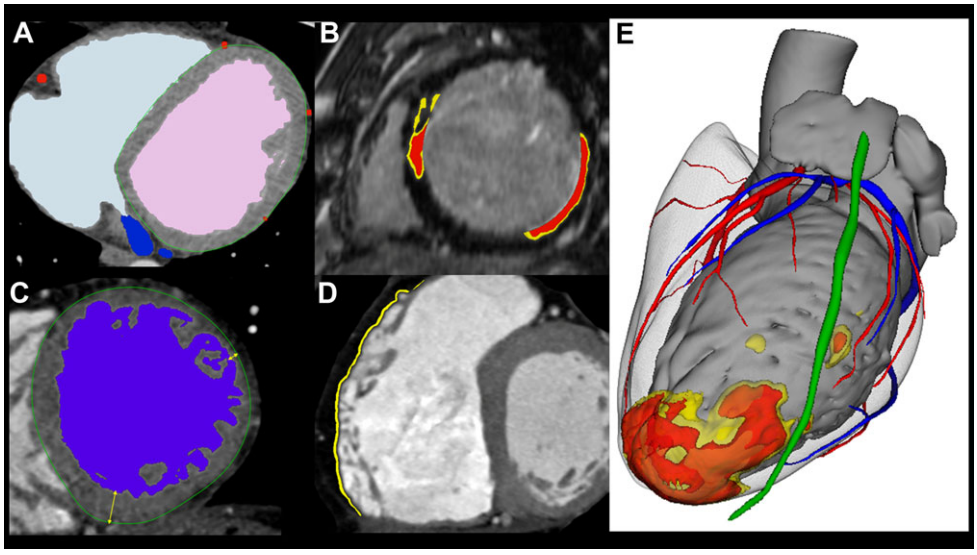


**Figure 2.** *Image processing strategy. A: Imaging is used to segment the cardiac chambers, epicardium, coronary sinus, as well as coronary arteries and left phrenic nerve in case of epicardial approach. In ICM and NICM patients, the structural substrate was segmented on imaging as areas of LGE on CMR (B), and/or areas of WT (<5 mm) on MDCT (C). In patients with ARVC, the structural substrate was segmented as areas of myocardial HA on MDCT (D). All segmentations were used to compute a 3D cardiac model (E; CMR and MDCT fusion: LV endocardium is shown in gray, epicardium in translucent white, dense scar from CMR in orange, gray zone in yellow, coronary arteries in red, coronary sinus in blue, left phrenic nerve course in green). For a high quality, full color version of this figure, please see Journal of Cardiovascular Electrophysiology's website: www.wileyonlinelibrary.com/journal/jce*

### *Relationship Between Imaging Substrate/Low Voltage and LAVA*

The results of EP substrate mapping are shown in Table 3. A total of 5313 LAVA was found. The prevalence of endocardial LAVA was higher in ICM than NICM and ARVC (94% vs. 55% and 68%, $P < 0.01$ and $P = 0.03$), while no such difference was found on the epicardium (89%, 89%, and 100% for ICM, NICM, and ARVC, respectively). LVZ identified 90% of LAVA. The agreement between LAVA and LVZ was lower in NICM than in ICM and ARVC (74% vs. 96% and 96%, $P < 0.001$ and $P < 0.001$). The agreement between imaging substrate and LAVA according to each VT etiology and each imaging modality is illustrated in Figure 4. Imaging substrate identified 85% of LAVA. The agreement

**TABLE 3**
Procedural Results

| | Total (N = 116) | ICM (N = 67) | NICM (N = 30) | ARVC (N = 19) | P-Value |
|---|---|---|---|---|---|
| Carto/Navx | 81/35 | 49/18 | 19/11 | 13/6 | *0.463<br>†0.909<br>‡0.955 |
| Epicardial approach, n | 66 (57%) | 25 (37%) | 22 (73%) | 19 (100%) | *0.002<br>†<0.001<br>‡0.016 |
| Endocardium | | | | | |
| Mapping points, n/pt. | 342 (208–553) | 370 (236–724) | 213 (157–291) | 450 (301–755) | *<0.001<br>†0.622<br>‡<0.001 |
| LVZ area, $cm^2$ | 50 (24–85) | 59 (33–91) | 19 (0–40) | 58 (26–74) | *<0.001<br>†0.263<br>‡<0.001 |
| Presence of LAVA, n | 91/113 (81%) | 61/65 (94%) | 16/29 (55%) | 13/19 (68%) | *<0.001<br>†0.008<br>‡0.387 |
| LAVA points, n/pt. | 24 (16–40) | 28 (20–42) | 18 (13–41) | 16 (9–23) | *<0.001<br>†0.545<br>‡0.132 |
| Epicardium | | | | | |
| Mapping points, n/pt. | 580 (337–1,042) | 432 (338–911) | 666 (291–1,100) | 582 (414–1,030) | *0.456<br>†0.649<br>‡0.766 |
| LVZ area, $cm^2$ | 70 (41–113) | 65 (43–96) | 40 (17–88) | 120 (75–139) | *0.242<br>†0.002<br>‡<0.001 |
| Presence of LAVA, n | 57/66 (86%) | 20/25 (80%) | 18/22 (82%) | 19/19 (100%) | *1.000<br>†0.060<br>‡0.111 |
| LAVA points, n/pt. | 28 (18–53) | 19 (16–30) | 43 (26–56) | 32 (18–63) | *0.172<br>†0.551<br>‡0.285 |
| Complete LAVA elimination, n | 71/111 (64%) | 41/64 (64%) | 14/28 (50%) | 16/19 (84%) | *0.251<br>†0.158<br>‡0.029 |
| VT non-inducibility, n | 22 (19%) | 52 (78%) | 25 (83%) | 17 (89%) | *0.597<br>†0.340<br>‡0.691 |
| Total RF duration, minutes | 34 (23–51) | 34 (23–56) | 31 (20–47) | 35 (24–44) | *0.114<br>†0.556<br>‡0.410 |
| Epicardial ablation, n | 47/66 (71%) | 15/25 (60%) | 18/22 (82%) | 14/19 (74%) | *0.123<br>†0.522<br>‡0.709 |
| Epicardial RF duration, minutes | 8.5 (0–18) | 2 (0–8.5) | 18 (9–25) | 9 (0.3–15) | *0.002<br>†0.254<br>‡0.039 |
| Procedure time, minutes | 282 ± 75 | 269 ± 73* | 295 ± 92 | 302 ± 41* | *0.201<br>†0.016<br>‡0.766 |

*ICM versus NICM, †ICM versus ARVC, ‡NICM versus ARVC.
LAVA = local abnormal ventricular activity; LVZ = low-voltage zone; RF = radiofrequency.

between LAVA and imaging substrate was lower in NICM than in ICM and ARVC (72% vs. 90% and 90%, $P < 0.0001$ and $P < 0.0001$). In ICM and NICM, the agreement between imaging and LAVA was higher when using CMR than MDCT (92% vs. 88%, $P = 0.026$ in ICM; 88% vs. 72%, $P < 0.001$ in NICM). This relationship was similarly observed in 25 patients who underwent both MDCT and CMR (18 in ICM, 7 in NICM). In this population, the agreement between imaging and LAVA was higher from CMR than from MDCT data (total population: 90% vs. 75%, $P < 0.0001$; ICM: 91% vs. 79%, $P < 0.0001$, NICM: 88% vs. 61%, $P < 0.0001$).

In the total population, imaging substrate correctly identified 433/511 (85%) of LAVA located in normal voltage areas, whereas voltage mapping correctly identified 705/783 (90%) of LAVA located outside the imaging substrate. The combination of voltage mapping and imaging substrate led to the identification of 5235/5313 (99%) of LAVA. Typical examples of image-guided VT ablation in patients with ICM, NICM, and ARVC are shown in Figure 5.

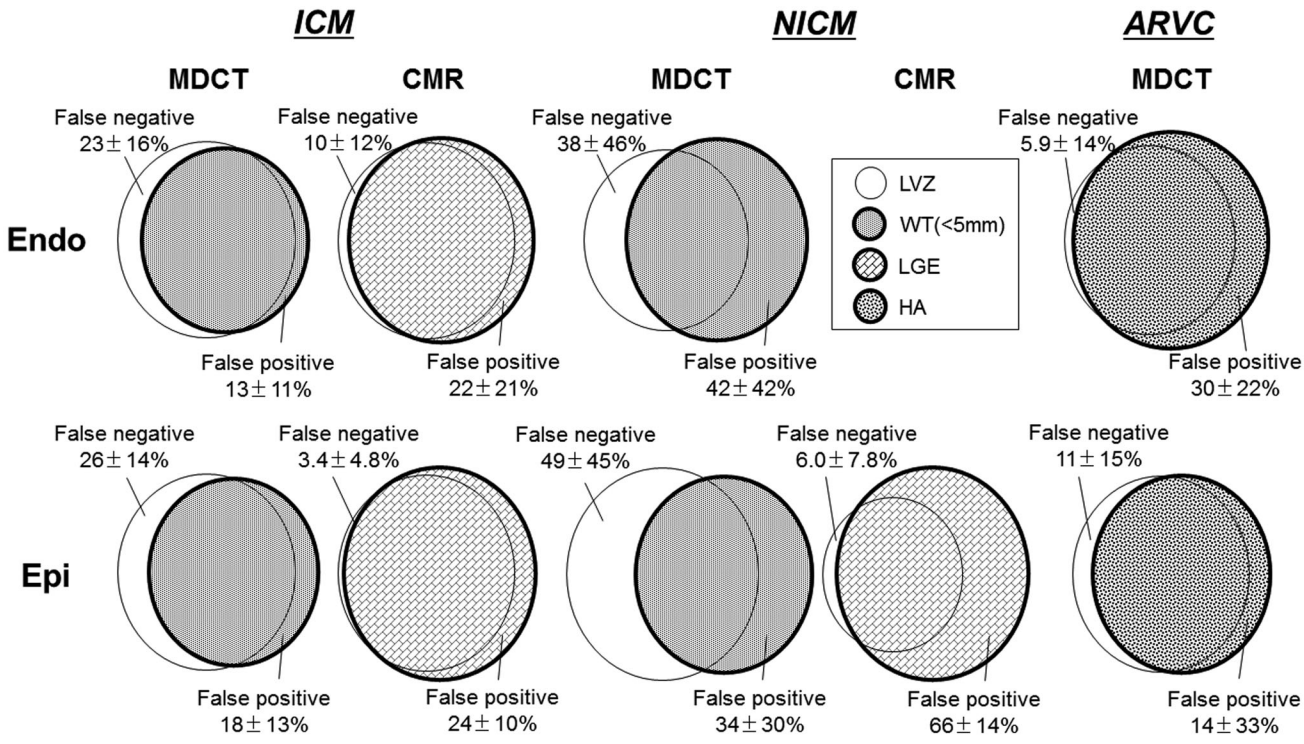


**Figure 3.** *Agreement between structural substrate on imaging and voltage mapping. The agreement is shown on both the endocardium and epicardium according to each VT etiology and each imaging modality. False-positive and false-negative areas are expressed in % of imaging substrate area. Endocardial analysis on CMR in NICM patients was excluded because all of the 9 patients with CMR had no LVZ and LAVA on the endocardium in this population. HA = hypo-attenuation; LGE = late gadolinium-enhancement; LVZ = low voltage zone; WT = wall thinning.*

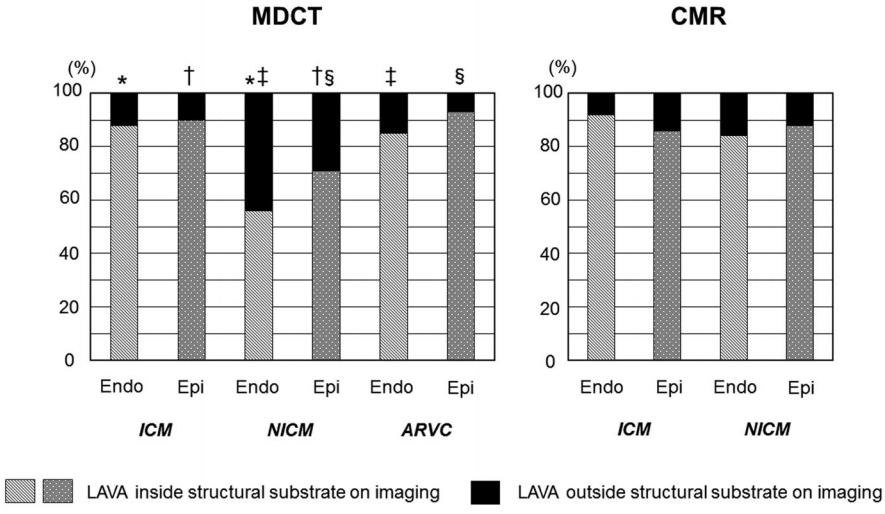


**Figure 4.** *Agreement between structural substrate on imaging and LAVA during SR. The % of LAVAs within imaging substrate is shown on both the endocardium and epicardium according to each VT etiology and each imaging modality.* $^{*}P < 0.0001$, $^{\dagger}P < 0.0001$, $^{\ddagger}P < 0.0001$, $^{\S}P < 0.0001$.

### *Ablation and Outcome*

One hundred and eighty-four sustained VTs were observed (cycle length 394 ± 123 milliseconds), 44 (24%) of which were terminated during RF application (24 ICM, 8 NICM, 12 ARVC). Thirty-nine (89%) of these termination sites were located within the imaging substrate, including 36 (82%) at the border zone, i.e., within 1 cm from margin (Supporting Fig. S1). LAVA was observed during SR at all termination sites. Complete LAVA elimination was achieved in 71/112 (63%) patients. Incomplete LAVA elimination was more frequent in NICM than in ARVC (50% vs. 16%, P = 0.03) but not significantly different than in ICM (50% vs. 36%, P = 0.30). Coronary angiography and phrenic pacing before epicardial RF applications were performed in 13/66 (20%) and 18/66 (27%) patients, respectively. LAVA could not be eliminated due to the proximity of CAs or PN in 9 (8%) patients (8 NICM, 1 ARVC), and due to pericardial bleeding in 5 (5%) patients (2 NICM, 3 ICM). In 4 patients with no LAVA (3 ICM, 1 NICM), sustained VT could not be induced and pace-map-based ablation was performed. Major complications occurred in 2 (1.7%) patients (cardiac tamponade requiring surgery and complete atrioventricular block). Minor complications occurred in 6 (5.2%) patients (4 pericardial bleedings, 2 hemi-blocks). After a median follow-up of 522 [350–730] days, VT recurrence

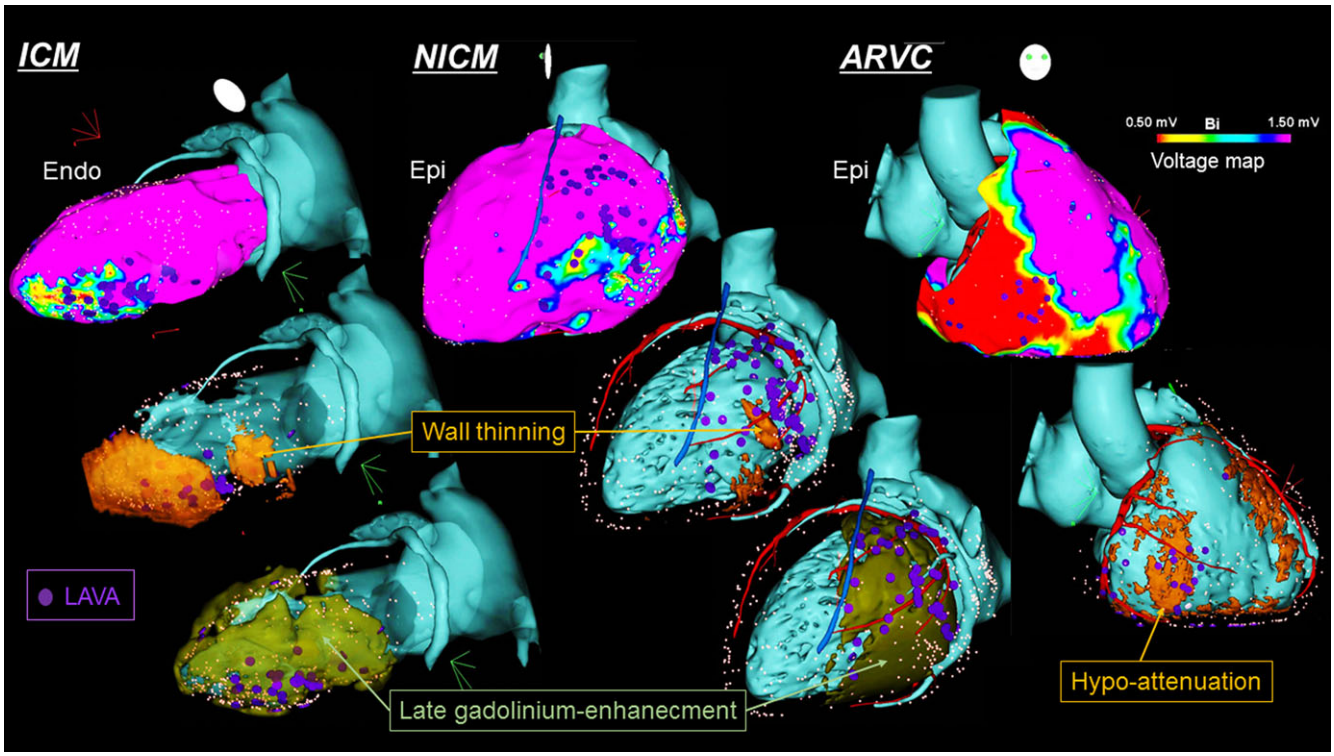


**Figure 5.** *Examples of image-guided VT ablation in patients with ICM, NICM, and ARVC. A case of ICM (male, 56 years) is shown in the first column, NICM (male, 41 years) in the second column, and ARVC (male, 60 years) in the third column. Bipolar voltage maps are shown on the top row, MDCT-derived substrate in orange on the second row, and CMR-derived substrate in green on the third row. Blue dots indicate LAVA. Blue line in the second column indicates the course of the left phrenic nerve. For a high quality, full color version of this figure, please see Journal of Cardiovascular Electrophysiology's website: www.wileyonlinelibrary.com/journal/jce*

was observed in 35 (30%) patients, and death from cardiac causes in 13 (11%). The rates of VT recurrence and cardiac death were higher in NICM than in ICM and ARVC ($P = 0.0003$ and $P = 0.03$) (Supporting Fig. S2). In patients with ICM and NICM, incomplete LAVA elimination and LVEF were independent predictors of VT recurrence at multivariable analysis (LVEF; HR: 0.96, CI: 0.92–0.99, $P = 0.02$, incomplete LAVA elimination; HR: 2.25, CI: 1.06–4.77, $P = 0.04$).

### *Impact of Image Integration on Procedural Management*

Pre-procedural imaging influenced the decision to perform epicardial access in 38 (33%) patients (6 ICM [9%], 13 NICM [43%], 19 ARVC [100%]). Epicardial LAVAs were found in all of these patients. After image registration, the integration of structural substrate specifically motivated additional mapping in 66 (57%) patients (34 ICM [51%], 19 NICM [63%], 13 ARVC [68%]), in which additional LAVA was found in all cases. Epicardial ablation strategy was modified due to the proximity of CAs and PN as displayed from imaging in 50 (43%) patients (15 ICM [22%], 18 NICM [60%], 17 ARVC [89%]). Image integration was categorized as not helpful in 34 (29%) patients, helpful in 57 (49%), and extremely helpful in 25 (22%). Image integration was more likely to be helpful in NICM and ARVC than in ICM (impact score $1.6 \pm 1.3$ and $2.6 \pm 0.6$ vs. $0.8 \pm 0.7$, $P = 0.003$ and $P < 0.001$). It was also more helpful in epicardial approaches than endocardial approach only (impact score $1.9 \pm 1.1$ vs. $0.5 \pm 0.5$, $P < 0.0001$). No significant difference was found between procedures with versus without CMR (impact score $1.3 \pm 1.1$ vs. $1.3 \pm 1.1$, $P = 0.89$).

## Discussion

This study is to our knowledge the first reporting on a systematic use of image integration during catheter ablation for scar-related VT of various etiologies. The main findings are that (i) the integration of high-resolution anatomical and scar imaging data is feasible with processing times compatible with routine practice, (ii) imaging provides valuable information on VT substrate that is complementary to that provided by voltage mapping, (iii) the agreement between the imaging substrate and LAVA is lower in NICM than in ICM and ARVC, and (iv) real-time image integration significantly impacts the procedural management in most patients, particularly in ARVC, NICM, and patients undergoing epicardial ablation.

### *Feasibility of Image Integration for VT Ablation*

The characteristics of the studied population are representative of typical cases undergoing VT ablation.[18,19] This study was made feasible thanks to the development of dedicated software enabling the integration of relevant patient-specific data on cardiac anatomy and myocardial structural substrate. Current commercialized software only enables the integration of gross anatomy of cardiac chambers, but the segmentation of CAs and left PN and the multimodal characterization of scar are not supported. To accommodate the broad spectrum of VT etiologies we used multiple imaging modalities to delineate substrate, i.e., WT or HA from MDCT, and LGE from CMR. These segmentation methods have been validated in past studies.[6,10,12] In our center, the processing of imaging data is performed

by technicians, aiming at rendering in 3D the report provided by the physician. The total processing time is consistently below 1 hour, and therefore compatible with routine practice.

### *Relationship Between Imaging and Procedural Results*

This study shows that the structural substrate defined by imaging identifies the vast majority of LAVA and critical VT isthmuses. The agreement between the imaging substrate and LAVA was particularly high in ICM and ARVC, however, lower in NICM. The results relating to ICM and ARVC are consistent with previous reports.[5,6,12] The lower performance of imaging in NICM patients may relate to limitations of imaging in identifying focal scar in early dilated cardiomyopathy.[20]

The performance of voltage mapping in identifying LAVA was found to be similar to that of imaging, with the same limitations in NICM. However, a substantial mismatch was found between substrate as defined on imaging and on voltage mapping. Areas with substrate on imaging and normal voltage can be explained by the limitations of voltage mapping in identifying non-transmural or intramural scar, due to far field signal.[5] Areas with low voltage and no imaging substrate can be explained by (i) false-positive low voltage due to poor contact or epicardial fat,[21] (ii) limitations of MDCT in assessing ischemic scars with limited impact on wall thickness,[6] (iii) limitations of imaging in assessing diffuse scar in NICM,[20] and (iv) registration error for image integration because of breathing or heart beating.

Interestingly, the information provided by voltage and imaging appears to be complementary, with 99% of LAVA identified when combining LVZ and imaging substrate areas. This information is critical as it substantiates the use of a multimodal definition of the substrate on combined voltage and imaging data, the operator being confident that the targeting of these areas ensures that the entire VT substrate is treated. This strategy might impact patient outcome as complete LAVA elimination was found to be an independent predictor of VT recurrence in the present work, which is consistent with a prior study.[2]

### *Impact of Image Integration on Procedural Management*

A number of prior studies have reported agreement between imaging and VT substrate.[4-7,12,22] However, most of these reports were derived from post hoc analyses on limited series of patients. Our large series showed that image integration impacted procedural management. Specifically, image integration motivates additional mapping to increase the density of points in areas exhibiting abnormal imaging findings. Further, imaging influences the decision to undertake an epicardial approach. Overall, image integration enhances the ability to identify LAVA that would otherwise have been missed, which is particularly relevant as complete LAVA elimination is an important determinant of VT recurrence.[2] It is important to note that in contrast to NICM and ARVC, image integration offers less additional benefit in ICM, as there is a good correlation between LVZ area and imaging substrate (WT-MDCT and LGE-CMR).

Of note in the present study is that the rates of VT recurrence and cardiac death were lower than previous reports, data in scar-related VT.[19,23] Besides treatment efficiency, image integration may impact safety. To prevent risks of CAs and PN damage during epicardial ablation, current guidelines recommend the use of coronary angiography and phrenic pacing.[24] However, it may not be convenient or possible to apply these methods before and after each RF delivery. Therefore, the ability to visualize CAs and PN image integration might obviate the need for repeated iodine contrast injections, and time-consuming pacing protocols. Indeed, only 20–30% of cases with epicardial ablation needed coronary angiography and phrenic pacing before RF application in this study.

### *Study Limitations*

The first limitation of this study is the absence of a control group with no image integration to document an impact on patient outcome (including clinical outcome, procedural time, appropriate indication of epicardial approach, accuracy of identification of LAVA, and incidence of complications). Although this study demonstrates that a substantial number of ablation targets would have been missed in the absence of image integration, a potential improvement of treatment efficiency should be confirmed by comparative studies. Second, the utility of imaging to determine the need for epicardial access was not assessed in isolation. The decision was influenced by multiple criteria. Therefore, while we demonstrated a strong correlation between imaging substrate and epicardial LAVA, further studies with blinded comparisons are necessary in order to more accurately define the role of imaging and potentially develop predetermined algorithms. The third limitation is related to the absence of systematic myocardial biopsy and CMR, and as a consequence to the lack of discrimination between NICM etiologies. However, focal scar is detected in more than half of this population, and even in patients with no focal substrate visible on imaging, image integration might still be useful to provide CAs and PN segmentations, because this population frequently requires epicardial ablation.[25] The fourth limitation is the limited prevalence of midwall LGE in the studied population. The relationship between midwall LGE and LAVA should be analyzed in future studies. Fifth, the impact of imaging on the procedural management was determined by the operator, which can be viewed as subjective. In addition, although initial mapping was blinded from imaging, operators often performed additional mapping after image integration to make sure that no abnormal myocardium was left unexplored. Therefore, the relationships between imaging and mapping data have to be analyzed knowing that mapping was partly guided by imaging, which likely impacted the reported correlations. Randomized studies should be conducted to relate image integration to stronger endpoints such as VT recurrence or procedural complications. Last, although CMR appears to be more efficient than MDCT in localizing VT substrate in ICM and NICM, we did not perform CMR in patients with ICDs, mostly for image quality reasons.[26] The superiority of CMR should thus be interpreted carefully, knowing that patients were not randomly assigned to MDCT or CMR modalities. However, recent developments in CMR acquisition have dramatically reduced ICD-related artifacts.[27] Therefore, future studies should evaluate whether the use of these methods further improves the image integration strategy.

## Conclusions

Image integration during VT ablation is feasible and provides an accurate localization of VT substrate, with processing times compatible with routine use. Image integration has a potential of improving the procedural management in most patients, particularly patients with ARVC and NICM, and in case of epicardial approach.

## References


1. Bogun F, Good E, Reich S, Elmouchi D, Igic P, Lemola K, Tschopp D, Jongnarangsin K, Oral H, Chugh A, Pelosi F, Morady F: Isolated potentials during sinus rhythm and pace-mapping within scars as guides for ablation of post-infarction ventricular tachycardia. J Am Coll Cardiol 2006;47:2013-2019.
2. Jaïs P, Maury P, Khairy P, Sacher F, Nault I, Komatsu Y, Hocini M, Forclaz A, Jadidi AS, Weerasooryia R, Shah A, Derval N, Cochet H, Knecht S, Miyazaki S, Linton N, Rivard L, Wright M, Wilton SB, Scherr D, Pascale P, Roten L, Pederson M, Bordachar P, Laurent F, Kim SJ, Ritter P, Clementy J, Haïssaguerre M: Elimination of local abnormal ventricular activities: A new end point for substrate modification in patients with scar-related ventricular tachycardia. Circulation 2012;125:2184-2196.
3. Harada T, Stevenson WG, Kocovic DZ, Friedman PL: Catheter ablation of ventricular tachycardia after myocardial infarction: Relation of endocardial sinus rhythm late potentials to the reentry circuit. J Am Coll Cardiol 1997;30:1015-1023.
4. Andreu D, Berruezo A, Ortiz-Perez JT, Silva E, Mont L, Borras R, de Caralt TM, Perea RJ, Fernandez-Armenta J, Zeljko H, Brugada J: Integration of 3D electroanatomicmaps and magnetic resonance scar characterization into the navigation system to guide ventricular tachycardia ablation. Circ Arrhythm Electrophysiol 2011;4:674-683.
5. Wijnmaalen AP, van der Geest RJ, van Huls van Taxis CF, Siebelink HM, Kroft LJ, Bax JJ, Reiber JH, Schalij MJ, Zeppenfeld K: Head-to-head comparison of contrast-enhanced magnetic resonance imaging and electroanatomical voltage mapping to assess post-infarct scar characteristics in patients with ventricular tachycardias: Real-time image integration and reversed registration. Eur Heart J 2011;32:104-114.
6. Komatsu Y, Cochet H, Jadidi A, Sacher F, Shah A, Derval N, Scherr D, Pascale P, Roten L, Denis A, Ramoul K, Miyazaki S, Daly M, Riffaud M, Sermesant M, Relan J, Ayache N, Kim S, Montaudon M, Laurent F, Hocini M, Haïssaguerre M, Jaïs P: Regional myocardial wall thinning at multidetector computed tomography correlates to arrhythmogenic substrate in postinfarction ventricular tachycardia: Assessment of structural and electrical substrate. Circ Arrhythm Electrophysiol 2013;6:342-350.
7. Bogun FM, Desjardins B, Good E, Gupta S, Crawford T, Oral H, Ebinger M, vPelosi F, Chugh A, Jongnarangsin K, Morady F: Delayed-enhanced magnetic resonance imaging in nonischemic cardiomyopathy: Utility for identifying the ventricular arrhythmia substrate. J Am Coll Cardiol 2009;53:1138-1145.
8. Marcus FI, McKenna WJ, Sherrill D, Basso C, Bauce B, Bluemke DA, Calkins H, Corrado D, Cox MG, Daubert JP, Fontaine G, Gear K, Hauer R, Nava A, Picard MH, Protonotarios N, Saffitz JE, Sanborn DM, Steinberg JS, Tandri H, Thiene G, Towbin JA, Tsatsopoulou A, Wichter T, Zareba W: Diagnosis of arrhythmogenic right ventricular cardiomyopathy/dysplasia: Proposed modification of the task force criteria. Circulation 2010;121:1533-1541.
9. Oakes RS, Badger TJ, Kholmovski EG, Akoum N, Burgon NS, Fish EN, Blauer JJ, Rao SN, DiBella EV, Segerson NM, Daccarett M, Windfelder J, McGann CJ, Parker D, MacLeod RS, Marrouche NF: Detection and quantification of left atrial structural remodeling with delayed-enhancement magnetic resonance imaging in patients with atrial fibrillation. Circulation 2009;119:1758-1767.
10. Cochet H, Komatsu Y, Sacher F, Jadidi AS, Scherr D, Riffaud M, Derval N, Shah A, Roten L, Pascale P, Relan J, Sermesant M, Ayache N, Montaudon M, Laurent F, Hocini M, Haïssaguerre M, Jaïs P: Integration of merged delayed-enhanced magnetic resonance imaging and multidetector computed tomography for the guidance of ventricular tachycardia ablation: A pilot study. J Cardiovasc Electrophysiol 2013;24:419-426.
11. Yamashita S, Sacher F, Mahida S, Berte B, Lim HS, Komatsu Y, Amraoui S, Denis A, Derval N, Laurent F, Montaudon M, Hocini M, Haïssaguerre M, Jaïs P, Cochet H: The role of high-resolution image integration to visualize left phrenic nerve and coronary arteries during epicardal ventricular tachycardia ablation. Circ Arrhythm Electrophysiol 2015;8:371-380.
12. Komatsu Y, Jadidi A, Sacher F, Denis A, Daly M, Derval N, Shah A, Lehrmann H, Park CI, Weber R, Arentz T, Pache G, Sermesant M, Ayache N, Relan J, Montaudon M, Laurent F, Hocini M, Haïssaguerre M, Jaïs P, Cochet H: Relationship between MDCT-imaged myocardial fat and ventricular tachycardia substrate in arrhythmogenic right ventricular cardiomyopathy. J Am Heart Assoc 2014;7;3. piii: e000935.
13. Amado LC, Gerber BL, Gupta SN, Rettmann DW, Szarf G, Schock R, Nasir K, Kraitchman DL, Lima JA: Accurate and objective infarct sizing by contrast-enhanced magnetic resonance imaging in a canine myocardial infarction model. J Am Coll Cardiol 2004;44:2383-2389.
14. Roes SD, Borleffs CJ, van der Geest RJ, Westenberg JJ, Marsan NA, Kaandorp TA, Reiber JH, Zeppenfeld K, Lamb HJ, de Roos A, Schalij MJ, Bax JJ: Infarct tissue heterogeneity assessed with contrast-enhanced MRI predicts spontaneous ventricular arrhythmia in patients with ischemic cardiomyopathy and implantable cardioverter defibrillator. Circ Cardiovasc Imaging 2009;2:183-190.
15. Cochet H, Denis A, Komatsu Y, Jadidi AS, Aït Ali T, Sacher F, Derval N, Relan J, Sermesant M, Corneloup O, Hocini M, Haïssaguerre M, Laurent F, Montaudon M, Jaïs P: Automated quantification of right ventricular fat at contrast-enhanced cardiac multidetector CT in arrhythmogenic right ventricular cardiomyopathy. Radiology 2015;275:683-691.
16. Lim HS, Sacher F, Cochet H, Berte B, Yamashita S, Mahida S, Zellerhoff S, Komatsu Y, Denis A, Derval N, Hocini M, Haïssaguerre M, Jaïs P: Safety and prevention of complications during percutaneous epicardial access for the ablation of cardiac arrhythmias. Heart Rhythm 2014;11:1658-1665.
17. Andreu D, Ortiz-Pérez JT, Boussy T, Fernández-Armenta J, de Caralt TM, Perea RJ, Prat-González S, Mont L, Brugada J, Berruezo A: Usefulness of contrast-enhanced cardiac magnetic resonance in identifying the ventricular arrhythmia substrate and the approach needed for ablation. Eur Heart J 2014;35:1316-1326.
18. Wissner E, Stevenson WG, Kuck KH: Catheter ablation of ventricular tachycardia in ischaemic and non-ischaemic cardiomyopathy: Where are we today? A clinical review. Eur Heart J 2012;33:1440-1450.
19. Philips B, Madhavan S, James C, Tichnell C, Murray B, Dalal D, Bhonsale A, Nazarian S, Judge DP, Russell SD, Abraham T, Calkins H, Tandri H: Outcomes of catheter ablation of ventricular tachycardia in arrhythmogenic right ventricular dysplasia/cardiomyopathy. Circ Arrhythm Electrophysiol 2012;5:499-505.
20. McCrohon JA, Moon JC, Prasad SK, McKenna WJ, Lorenz CH, Coats AJ, Pennell DJ: Differentiation of heart failure related to dilated cardiomyopathy and coronary artery disease using gadolinium-enhanced cardiovascular magnetic resonance. Circulation 2003;108:54-59.
21. Desjardins B, Morady F, Bogun F: Effect of epicardial fat on electroanatomical mapping and epicardial catheter ablation. J Am Coll Cardiol 2010;56:1320-1327.
22. Estner HL, Zviman MM, Herzka D, Miller F, Castro V, Nazarian S, Ashikaga H, Dori Y, Berger RD, Calkins H, Lardo AC, Halperin HR: The critical isthmus sites of ischemic ventricular tachycardia are in zones of tissue heterogeneity, visualized by magnetic resonance imaging. Heart Rhythm 2011;8:1942-1949.
23. Stevenson WG, Wilber DJ, Natale A, Jackman WM, Marchlinski FE, Talbert T, Gonzalez MD, Worley SJ, Daoud EG, Hwang C, Schuger C, Bump TE, Jazayeri M, Tomassoni GF, Kopelman HA, Soejima K, Nakagawa H; Multicenter Thermocool VT Ablation Trial Investigators: Irrigated radiofrequency catheter ablation guided by electroanatomic mapping for recurrent ventricular tachycardia after myocardial infarction: The multicenter thermocool ventricular tachycardia ablation trial. Circulation 2008;118:2773-2782.
24. Aliot EM, Stevenson WG, Almendral-Garrote JM, Bogun F, Calkins CH, Delacretaz E, Della Bella P, Hindricks G, Jaïs P, Josephson ME, Kautzner J, Kay GN, Kuck KH, Lerman BB, Marchlinski F, Reddy V, Schalij MJ, Schilling R, Soejima K, Wilber D: European Heart Rhythm Association (EHRA); Registered Branch of the European Society of Cardiology (ESC); Heart Rhythm Society (HRS); American College of Cardiology (ACC); American Heart Association (AHA). EHRA/HRS Expert Consensus on Catheter Ablation of Ventricular Arrhythmias: Developed in a partnership with the European Heart Rhythm Association (EHRA), a Registered Branch of the European Society of Cardiology (ESC), and the Heart Rhythm Society (HRS); in collaboration with the American College of Cardiology (ACC) and the American Heart Association (AHA). Heart Rhythm 2009;6:886-933.
25. Cano O, Hutchinson M, Lin D, Garcia F, Zado E, Bala R, Riley M, Cooper J, Dixit S, Gerstenfeld E, Callans D, Marchlinski FE:

Electroanatomic substrate and ablation outcome for suspected epicardial ventricular tachycardia in left ventricular non ischemic cardiomyopathy. J Am Coll Cardiol 2009;54:799-808.
26. Mesubi O, Ahmad G, Jeudy J, Jimenez A, Kuk R, Saliaris A, See V, Shorofsky S, Dickfeld T: Impact of ICD artifact burden on late gadolinium enhancement cardiac MR imaging in patients undergoing ventricular tachycardia ablation. Pacing Clin Electrophysiol 2014;37:1274-1283.
27. Stevens SM, Tung R, Rashid S, Gima J, Cote S, Pavez G, Khan S, Ennis DB, Finn JP, Boyle N, Shivkumar K, Hu P: Device artifact reduction for magnetic resonance imaging of patients with implantable cardioverter-defibrillators and ventricular tachycardia: Late gadolinium enhancement correlation with electroanatomic mapping. Heart Rhythm 2014;11:289-298.

## Supporting Information

Additional supporting information may be found in the online version of this article at the publisher's website:

**Figure S1.** VT termination at the border of MDCT-defined structural substrate in an ischemic patient. (A)Endocardial voltage map in the LV during SR. LVZ was identified in inferior-apex aspect with LAVA (white tag). Intracardiac recordings on RF distal at the red tag (VT termination site) demonstrated abnormal discrete potentials (LAVA) located after LV far field signal within QRS complex during SR (arrow). (B) Twelve-lead ECG during clinical VT with negative axis and negative concordance throughout the precordial leads (cycle length: 350 milliseconds). (C) Activation map during clinical VT. VT originated from infero-apical LV. Intracardiac recordings demonstrated mid-diastolic potentials during VT (asterisk) and concealed fusion entrainment with good postpacing interval at the red tag point. VT terminated after 4 seconds of RF application at this site. (D) Activation map during clinical VT with integrated imaging from CT (WT<5 mm). VT termination site (red tag) located 5 mm from the border of imaging substrate. CS indicates coronary sinus; RFd, radiofrequency distal; RFp, radiofrequency proximal.

**Figure S2.** Kaplan–Meier analysis for VT recurrence and cardiac death after image-guided VT ablation.